Supramolecular assembly of an amphiphilic Gd^{III} chelate: tuning the reorientational correlation time and the water exchange rate

Susana Torres [a], José A. Martins *[a], João P. André *[a], Carlos F.G.C. Geraldes [b], André E. Merbach [c], Éva Tóth *[c]

[a] S. Torres, Dr. J. A. Martins (jmartins@quimica.uminho.pt), Dr. J. P. André (jandre@quimica.uminho.pt)
Centro de Química, Campus de Gualtar, Universidade do Minho, 4710-057 Braga, Portugal.

Fax: (351) 253-678983

[b] Prof. Dr. C. F.G.C. Geraldes

Departamento de Bioquímica, Centro de Espectroscopia RMN e Centro de Neurociências e Biologia Celular, Faculdade de Ciências e Tecnologia, Universidade de Coimbra, 3001-401 Coimbra, Portugal.

[c] Prof. Dr. A. E. Merbach, Dr. É. Tóth (eva.jakabtoth@epfl.ch)
Laboratoire de Chimie Inorganique et Bioinorganique, École Polytechnique Fédérale de Lausanne, Switzerland.

Dedicated to Professor *Ernő Brücher* on the occasion of his 70th birthday.

Keywords: Micelles, Imaging Agents, Gadolinium, Water Exchange, Steric Compression, MRI, CMC

Abstract

In this paper we report the synthesis and the characterization of the novel ligand H_5EPTPA-C16 ((hydroxymethylhexadecanoyl ester)ethylenepropylenetriaminepentaacetic acid). This ligand was designed to chelate the Gd^{III} ion in a kinetically and thermodynamically stable way while ensuring an increased water exchange rate (k_{ex}) on the Gd^{III} complex due to steric compression around the water binding site. The attachment of a palmitic ester unit to the pendant hydroxymethyl group on the ethylenediamine bridge yields an amphiphilic conjugate that forms micelles in aqueous solution with a long tumbling time (τ_R). The critical micelle concentration (CMC = 0.34 mM) of the amphiphilic $[Gd(EPTPA\text{-}C16)(H_2O)]^{2-}$ chelate was determined by variable concentration proton relaxivity measurements. A global analysis of the data obtained in variable temperature and multiple field ^{17}O NMR, and ^{1}H NMRD measurements allowed the determination of parameters governing relaxivity for $[Gd(EPTPA\text{-}C16)(H_2O)]^{2-}$; this is the first time that paramagnetic micelles with optimized water exchange are investigated. The water exchange rate was found to be $k_{ex}^{298} = 1.7\times10^8$ s^{-1}, very similar to that previously reported for the nitrobenzyl derivative $[Gd(EPTPA\text{-}bz\text{-}NO_2)(H_2O)]^{2-}$ ($k_{ex}^{298} = 1.5\times10^8$ s^{-1}). The rotational dynamics of the micelles was analysed using the Lipari-Szabo approach. The micelles formed in aqueous solution show a considerable flexibility, with a local rotational correlation time of the Gd^{III} segments, τ_{lO}^{298} = 330 ps, being much shorter than the global rotational correlation time of the supramolecular aggregates, τ_{gO}^{298} = 2100 ps. This internal flexibility of the micelles is responsible for the only limited increase of the proton relaxivity observed on micelle formation (r_1 = 22.59 $mM^{-1}s^{-1}$ for the micelles vs. 9.11 $mM^{-1}s^{-1}$ for the monomer chelate (20 MHz; 25°C)).

Introduction

The success of magnetic resonance imaging (MRI) as a clinical diagnostic technique is largely related to the use of paramagnetic contrast agents which improve the contrast between normal and diseased tissues. Trivalent gadolinium chelates have shown to be the most suitable MRI contrast agents (CAs) [1-7]. One of the big challenges in the development of new CAs is the improvement of their relaxivity and their capability to target certain organs and tissues which would allow the clinical use of lower doses [8-9] (proton relaxivity is defined as the paramagnetic longitudinal proton relaxation rate enhancement due to one millimolar concentration of the agent). Theory predicts that slow rotation of the chelates in solution (long τ_R values) and fast water exchange between the ion coordination sphere and the bulk water (high $k_{ex}=1/\tau_m$ values, where τ_m is the lifetime of the water molecule in the coordination sphere) will lead to higher relaxivities [4,6]. Upon attachment of low molecular weight Gd^{III}-chelates to macromolecules, the rotation slows down and the relaxivity increases. However this increase is usually far from being optimal (r_{1max} ~100 $mM^{-1}s^{-1}$ for a q=1 complex at 20-60 MHz proton Larmor frequency) because either the bound chelate is too flexible (internal motions dominate) or water exchange becomes limiting ($\tau_m > T_{1M}$) [2,6].

Several approaches have been attempted to increase τ_R values in the search for high relaxivities. These involved the formation of covalent or non-covalent conjugates between the paramagnetic chelate and slowly moving substrates (dendrimers [10], proteins [11]; carbohydrates [12]). An appealing alternative way to increase τ_R is through self-assembly of amphiphilic Gd^{III}-chelates forming micelles [13]. Many of these Gd^{III}-containing assemblies behave as colloidal carriers which, in addition to the increased relaxivities, show good pharmacological characteristics [14]. They can be efficiently taken up by macrophage-rich tissue undergoing endocytosis/phagocytosis (liver and spleen) [15,16] and have proved to be

useful for diagnostic purposes [15]. Long-circulating colloidal systems with entrapped radiopharmaceuticals or CAs have been successful in blood-pool imaging [17-19].

Several Gd^{III}-based micellar systems have been designed and characterized [13, 20, 21]. In these systems the relaxivities were considerably improved due to the longer tumbling times in solution but low water exchange rates seriously cut back the relaxivity gain.

The chelate $[Gd(TRITA)(H_2O)]^-$ (H_4TRITA = 1,4,7,10-tetraazacyclotridecane-N,N',N'',N'''-tetraacetic acid) was reported to have a fast water exchange due to steric compression around the water binding site. The increased steric crowding in this chelate is achieved by replacing an ethylene bridge of $DOTA^{4-}$ (H_4DOTA = 1,4,7,10-tetraazacyclododecane-N,N',N'',N'''-tetraacetic acid) by a propylene bridge [22]. The same strategy proved successful in accelerating water exchange in the Gd^{III}-chelates of modified $DTPA^{5-}$ ligands (H_5DTPA = diethylenetriamine-N,N,N',N'',N''-pentaacetic acid). These ligands present one propylene bridge (H_5EPTPA = ethylenepropylenetriamine-N,N,N',N'',N''-pentaacetic acid) instead of the original ethylene bridge, or one coordinating propionate arm (H_5DTTA-N'prop = diethylenetriamine-N,N,N'',N''-tetraacetic-N'-propionic acid) instead of the acetate arm of $DTPA^{5-}$ [23]. A different system displaying fast water exchange at the Gd^{III} ion is based on a mono-amide DOTA complex, as demonstrated by Parker and co-workers [24].

With the objective of slowing down the rotation, the fast exchanging $[Gd(EPTPA)(H_2O)]^{2-}$ chelate has been attached to different generations (5,7 and 9) of PAMAM dendrimers [25]. A combined ^{17}O NMR and proton relaxivity study of these systems showed that, in contrast to previously reported dendrimeric Gd^{III} complexes, the proton relaxivity was indeed not at all limited by slow water exchange.

In this paper we report the synthesis of the new ligand H_5EPTPA-C16 ((hydroxymethylhexadecanoyl ester)ethylenepropylenetriaminepentaacetic-acid)), which was designed to chelate the Gd^{III} ion in a kinetically and thermodynamically stable way [23] while

displaying a simultaneous optimization of the rotational correlation time and the water exchange rate and hence a higher relaxivity. The tumbling time of the chelate is slowed down upon attachment of a C-16 lipophilic chain to the -CH_2OH pendant group through ester bond formation. Due to the capability of this amphiphilic species to form micelles in solution, its τ_R value will be substantially increased. In addition, the τ_m value of the Gd^{III}-chelate is optimized in comparison to commercial chelates such as $[Gd(DTPA)(H_2O)]^{2-}$, as a consequence of an increased steric compression in the coordination sphere of the metal ion, brought about by the propylene bridge connecting two nitrogen atoms.

The critical micelle concentration (CMC) of the amphilic $[Gd(EPTPA\text{-}C16)(H_2O)]^{2-}$ chelate was determined by proton relaxivity measurements. In the aim of assessing the parameters that determine proton relaxivity, the water exchange rate and rotational correlation time in particular, we have carried out a variable temperature and multiple field ^{17}O NMR and ^{1}H NMRD study. The rotational dynamics of the micelles was described in terms of local and global motions, related to motions of the Gd^{III} segments and of the entire micelle, respectively, by using the Lipari-Szabo approach in the analysis of longitudinal NMR relaxation rates.

Results and Discussion

Synthesis

The new CA skeleton $EPTPA^{5-}$ has been proposed recently, which features a masked, pendant amine group on the ethylenediamine unit designed for conjugation to chemical moieties for targeting purposes and/or for the formation of macromolecular complexes.[23] In this paper we report a new synthetic route to the $EPTPA^{5-}$ skeleton bearing a hydroxymethyl group on the ethylenediamine unit (Scheme 1).

We envisaged that coupling a fatty acid to the hydroxymethyl group would generate the amphyphylic molecule **8** (EPTPA-C16) that would self-assemble in solution, thus increasing the tumbling time, and the relaxivity of its Gd^{III} complex.

The reductive amination of the Garner aldehyde **2** with the Boc-monoprotected diamine **3** is the key reaction in the construction of the EPTPA scaffold. The reducing agent sodium triacetoxyborohydride $NaBH(OAc)_3$ proved to be highly efficient [26]. The Garner aldehyde **2** was obtained through a high yielding three-step procedure from serine methyl ester hydrochloride **1** [27]. The fully protected triamine **4** was deprotected in quantitative yield in one step with a HCl 6 M / EtOH (1/1) mixture. The alkylation reaction required pre-titration of the aqueous triamine hydrochloride to neutral pH. The titration with Dowex 1X2-100-OH^- resin revealed to be a convenient procedure. The fully deprotected triamine **5** was of analytical purity and was carried through without further purification. Triamine **5** was alkylated with *t*Bu-bromoacetate in a standard procedure [23]. The fully alkylated material **6** was coupled to palmitic acid through the anhydride method. The resulting ester **7** was isolated as an adduct with an extra molecule of palmitic acid, as demonstrated by ^1H NMR spectroscopy. No attempts were made to purify the compound at this stage. We reasoned that it would be more efficient to carry this material through and to perform the final purification on the material at the fully deprotected stage. The deprotection with TFA/CH_2Cl_2 proceeded uneventfully, affording again the deprotected material as an adduct with an extra molecule of palmitic acid. The palmitic acid adduct was suspended in water and titrated to neutrality with aqueous KOH. This procedure allowed the removal of the insoluble potassium palmitate by filtration. The final compound was purified by RP C_8 chromatography eluting with H_2O/EtOH (100% H_2O → 100% EtOH) to afford the title material **8** in analytical purity. The hydroxymethyl group on the ethylenediamine unit originates from the amino acid serine. The synthesis started with the unnatural *R*-enantiomer. This synthetic route is not likely to have lead to racemization or

inversion of configuration on the stereogenic centre. Optical rotation measurements indicate that our final compound is optically active. Further studies are needed in order to confirm the absolute stereochemistry and the enantiomeric purity of the final compound **8**.

Determination of the critical micellar concentration (CMC)

The amphiphilic Gd^{III}-chelate is expected to behave as a surfactant in aqueous solution, i.e. to form macromolecular micellar structures. Micelle formation is characterized by the critical micellar concentration (CMC), the lowest concentration limit at which micelles start to appear in solution. We have determined the CMC value by means of ^1H relaxivity measurements (60 MHz and 25 ^oC). This procedure, previously established for paramagnetic micellar systems, is based on the variation of the water ^1H longitudinal relaxation rate with increasing concentrations of the Gd^{III}-chelate [21]. The measurements are performed at a frequency where the relaxivity is principally determined by rotation. Accordingly, micelle formation will result in a slower molecular tumbling and a concomitant increase of the observed proton relaxivity. At concentrations inferior to the CMC no aggregates form, and under these conditions, only the monomeric chelate contributes to the paramagnetic ^1H relaxation rate measured in the solution, which is given by Eq. (1):

$$R_1^{obs} - R_1^d = r_1^{n.a} \times C_{Gd} \qquad (1)$$

where R_1^d is the diamagnetic contribution to the longitudinal relaxation rate (the relaxation rate of pure water), $r_1^{n.a.}$ represents the relaxivity of the free, non-aggregated Gd^{III}-chelate (in $mmol^{-1}s^{-1}$) and c_{Gd} is the analytical Gd^{III} concentration.

At concentrations superior to the CMC, the measured relaxation rate is the sum of two contributions, one due to the chelate as monomer (free surfactant) present at a concentration given by the CMC and the other due to the aggregated form (micelles). The water ^1H relaxation rate measured for the paramagnetic solution can be then expressed as in Eq. (2):

$$R_1^{obs} - R_1^d = (r_1^{n.a} - r_1^a)\,CMC + r_1^a \times C_{Gd} \qquad (2)$$

where r_1^a is the relaxivity of the micellar (aggregated) form. The CMC is determined from the plot of the paramagnetic relaxation rates vs. the Gd^{III} concentration as shown in Figure 1, based on a simultaneous least-squares fit of the two straight lines. The slopes of these two lines define $r_1^{n.a.}$ and r_1^a, below and above the CMC, respectively. The values obtained were $r_1^{n.a.}$ = 7.79 $mmol^{-1}s^{-1}$ and r_1^a = 24.21 $mmol^{-1}s^{-1}$ (at 25 °C and 60 MHz). The CMC was found to be 0.34±0.02 mM, which, in a comparison to previously studied, similar amphiphilic Gd^{III} complexes with hydrocarbon chains, falls exactly into the range expected for a compound with a sixteen-carbon lipophilic tail (Figure 2) [21].

^{17}O NMR and ^{1}H NMRD measurements

In order to determine the water exchange rate and assess the rotational dynamics of the $[Gd(EPTPA\text{-}C16)(H_2O)]^{2-}$ chelate, we have measured variable-temperature, transverse and longitudinal ^{17}O relaxation rates and chemical shifts at two magnetic fields (4.7 and 9.4 T), at a concentration (0.027 mol/kg) which well exceeds the CMC. Thus we consider that the contribution of the monomeric form to the ^{17}O experimental data is negligible. Additionally, proton relaxivities were measured as a function of the Larmor frequency (NMRD profiles) at three different temperatures and EPR spectra were also recorded. Based on the analogy to the previously reported $[Gd^{III}(EPTPA\text{-}bz\text{-}NO_2)(H_2O)]^{2-}$, we assume $[Gd^{III}(EPTPA\text{-}C16)(H_2O)]^{2-}$ to be nine-coordinate with one inner sphere water molecule [23]. For the momomeric form of the chelate, we have determined the field-dependent proton relaxivities, $r_1^{n.a.}$, by ^{1}H NMRD measurements at a concentration of 0.2 mM (below the CMC -Figure 3). NMRD profiles were also recorded at c_{Gd} = 2 mM concentration (above the CMC). The relaxivities of the aggregated form, r_1^a, were calculated at each temperature and magnetic field (Figure 4c) by subtracting

the relaxation rate contribution of the monomer chelate, present at the concentration of the CMC (r_1^{na}×CMC), from the paramagnetic relaxation rate values measured at c_{Gd} = 2 mM concentration (R_1^{obs} - R_1^{d}), according to Eq. (3):

$$r_1^a = \left(R_1^{obs} - R_1^d - r_1^{na} \times CMC\right)/\left(c_{Gd} - CMC\right) \quad (3)$$

For the aggregated form of the chelate, we performed a simultaneous least-squares fit of the ^{17}O NMR, EPR and NMRD data, these latter calculated with Eq. (3). All the available experimental data (^{17}O NMR chemical shifts, $\Delta\omega_r$, longitudinal ($1/T_{1r}$) and transverse ($1/T_{2r}$) relaxation rates, the longitudinal proton relaxivities (r_1) and transverse electron spin relaxation rates, obtained from the EPR spectra) were analysed simultaneously. The data were fitted to the conventional Solomon-Bloembergen-Morgan theory [7], except for the description of the rotational dynamics (influencing both ^{17}O and ^{1}H longitudinal relaxation), for which we used the model-free Lipari-Szabo approach [28, 29] (see appendix for all equations). Indeed, the longitudinal ^{17}O relaxation rates show a distinct magnetic field dependence, which is always a clear indication of slow molecular motions and cannot be described by the common spectral density functions applied for small molecular weight chelates. According to the Lipari-Szabo approach, the modulation of the interaction that causes relaxation is the result of two statistically independent motions: a rapid local motion of the Gd^{III} segments, with a local rotational correlation time τ_l, and a slower global motion of the entire micellar aggregate, with a global rotational correlation time τ_g. The degree of spatial restriction of the local motion with regard to the global rotation is given by an additional model free parameter, S^2. For a totally free internal motion S^2 equals 0, while for a local motion which is exclusively correlated to the global motion, S^2=1.

Given the large number of parameters involved in the analysis of the ^{17}O NMR, EPR and NMRD data, some of them had to be fixed to common and physically meaningful values. For the distances we used r_{GdO} = 2.5 Å (Gd electron spin and ^{17}O nucleus distance), r_{GdH} = 3.1 Å

(Gd electron spin to ^{1}H nucleus distance) and a_{GdH} = 3.5 Å (closest approach of the bulk water protons to the gadolinium). The quadrupolar coupling constant for the bound water oxygen, $\chi(1+\eta^2/3)^{1/2}$, was fixed to 5.2 MHz [30]. The longitudinal ^{17}O relaxation is related to motions of the Gd-coordinated water oxygen vector, while the proton relaxation is determined by motions of the Gd-coordinated water proton vector. For the ratio of the rotational correlation time of the Gd - H_{water} and Gd - O_{water} vectors, τ_{RH}/τ_{RO}, similar values have been found for various small molecular weight monohydrated Gd^{III} complexes, both by experimental studies and MD simulations (τ_{RH}/τ_{RO} = 0.65±0.2) [30,31]. This τ_{RH}/τ_{RO} ratio, within the given error, is considered as a general value for the ratio of the two rotational correlation times. Thus, in the simultaneous analysis of ^{17}O NMR and NMRD data, we fixed the ratio of the local correlation times of the Gd - coordinated water proton vector (τ_{lH}) and the Gd - coordinated water oxygen vector (τ_{lO}) to 0.65. The global rotational correlation times obtained from oxygen and proton relaxation are identical ($\tau_{gO} = \tau_{gH}$). In the analysis, we fitted the rotational correlation times τ_{lO}^{298} and τ_{gO}^{298} characterizing the motion of the Gd - O_{water} vector. The experimental NMRD and ^{17}O NMR data and the fitted curves for $[Gd^{III}(EPTPA\text{-}C16)(H_2O)]^{2-}$ are presented in Figure 4. The X-band peak-to-peak EPR linewidths, not presented in Figure 4 but included in the fit, were between 440 Gauss (270 K) and 480 Gauss (316 K). The most relevant parameters obtained in the fit are shown in Table 1. For the electronic relaxation parameters we obtained the following values: τ_v^{298} = 43±5 ps and $\Delta^2 = (0.07\pm0.01)\times10^{20}$ s^{-2}; E_v was fixed to 1.0 kJ/mol. The value of the ^{17}O scalar coupling constant, essentially calculated from the ^{17}O chemical shifts, is $A/\hbar = -(3.1\pm0.3)\times10^6$ rad s^{-1}. The diffusion constant, D_{GdH}^{298}, and its activation energy, E_{DGdH}, were calculated to be (28±2) × 10^{-10} m^2 s^{-1} and (25±1) kJ mol^{-1}, respectively.

The NMRD profiles measured at three different temperatures for the non-aggregated chelate have also been fitted. Here, the rotational dynamics was described by the common spectral density functions of the Solomon-Bloembergen-Morgan theory, since the rotation is not slow

enough to require the Lipari-Szabo treatment. Due to the lack of ^{17}O NMR data directly on the monomer form, in the fit of the NMRD profiles we fixed the water exchange rate and the activation enthalpy to the values obtained for the micellar form (Table 1). The electronic parameters calculated are τ_v^{298} = 44±8 ps and Δ^2 = (0.08±0.01)×10^{20} s^{-2}; E_v was fixed to 1.0 kJ/mol. For the rotational correlation time, we obtained τ_{rH} = 200±30 ps, which corresponds to a value expected for a molecule of the given molecular weight (Table 2). The experimental NMRD profiles and the fitted curves are presented in Figure 3.

Water exchange rate and rotational dynamics

Table 2 shows proton relaxivity data, water exchange rates and rotational correlation times for a series of Gd^{III} compounds [13, 22, 23, 25, 34, 35], compared to the present results for $[Gd(EPTPA\text{-}C16)(H_2O)]^{2-}$ both in non-aggregated and aggregated forms. The water exchange rate of $[Gd(EPTPA\text{-}C16)(H_2O)]^{2-}$, k_{ex}^{298} = 170 × 10^6 s^{-1}, is consistent with the values obtained for analogue Gd^{III} EPTPA-derived chelates. In all of these compounds, steric compression around the water binding site leads to an accelerated water exchange in comparison to the DTPA-type Gd^{III} complexes. With regard to rotational dynamics, the large difference between the local (330 ps) and global (2100 ps) rotational correlation time of the aggregated $[Gd(EPTPA\text{-}C16)(H_2O)]^{2-}$ shows that the motion of a Gd^{III}-chelate segments (characterized by τ_l) is considerably faster than that of the whole micellar assembly (τ_g). This, together with the value of the order parameter, S^2 = 0.41, is a strong indication of the internal flexibility of the micelles. The parameter τ_g reflecting the global motion of the $[Gd(EPTPA\text{-}C16)(H_2O)]^{2-}$ micellar assembly is of the same order of magnitude as those reported for amphiphilic $[Gd(DOTAC_n)(H_2O)]^-$ complexes (n = 12, 14, 18) [35], but much smaller than the values for the large dendrimeric structures like Gadomer 17 [34] or G5-$(GdEPTPA)_{115}$ [25]. The τ_l value

for the $[Gd(EPTPA\text{-}C16)(H_2O)]^{2-}$ micelles is also similar to those for $[Gd(DOTAC_n)(H_2O)]^{-}$ (n = 12, 14, 18) [35], however shorter than that for Gadomer 17, which has a less flexible dendrimeric structure. On the other hand, the value of the order parameter, S^2 = 0.41 for $[Gd(EPTPAC16)(H_2O)]^{-}$ is only slightly smaller than S^2=0.5 calculated for Gadomer 17.

The interaction of $[Gd(EPTPAC16)(H_2O)]^{-}$ with human serum albumin was tested in a solution containing 4.5 % HSA. No increase in proton relaxivity was observed as compared to a sample without HSA (60 MHz), therefore we concluded that there is no significant interaction between the long chain and serum albumin.

Conclusion

We have devised a new, high-yielding synthetic strategy for the synthesis of a new chelator with the EPTPA skeleton featuring a hydroxymethyl group on the ethylenediamine unit. The hydroxymethyl group is available for direct conjugation to a plethora of chemical moieties through different linkages (ester, ether, phosphodiester, glycosidic bond, ether, etc). Moreover, the hydroxyl group may be easily converted to other functional groups functional e. g. aldehyde, carboxylic acid, azide, etc, leading to other convenient handles for conjugation. In this paper we have constructed a conjugate with a fatty acid to illustrate the concept. Furthermore, some linkages involving oxygen, e.g. ester and phosphodiester, are enzyme-labile, leading potentially to smart contrast agents.

On the basis of a rational design, we have prepared a new amphiphilic Gd^{III}-chelate, for which the parameters influencing relaxivity were obtained from a simultaneous analysis of NMRD, EPR and ^{17}O NMR data. As a result of micellar self-assembling in aqueous solution, the chelate has an increased rotational correlation time. In addition, due to a steric compression in the inner coordination sphere of the paramagnetic ion, both the amphiphilic monomer and the supramolecular micellar assembly display close to optimal water exchange rates, two orders of magnitude superior to the CAs in clinical use. However, the self-assembly

of the amphiphilic monomers leads only to a modest increase in relaxivity, as the rotational dynamics is strongly dominated by fast local motions of the Gd^{III} segments within the micelle. Clearly, as demonstrated by simulations, much higher relaxivities are achievable for chelates with water exchange rates of this order of magnitude, as long as the local rotational correlation times do not become limiting. The rigidification of the micelles is one possible route towards substantially higher relaxivities.

The lipophilic tail is attached to the chelate moiety through an ester bond, which will be likely cleaved in the presence of lipases. Such transformation of the chelate will significantly reduce the observed relaxivity. This behaviour could make the $[Gd(EPTPA\text{-}C16)(H_2O)]^{2-}$ chelate a potential responsive contrast agent, sensitive to the presence of lipases. Investigations in this perspective are in progress and will be reported in due course.

Experimental Section

Preparation of the complex: The Gd^{III} chelate of EPTPA-C16 was prepared by mixing equimolar amounts of $Gd(ClO_4)_3$ and the ligand in a 50 mM TRIS (tris(hydroxymethyl)amino –methane) buffer solution (pH around 7.0) or in 150 mM MES (2-[N-Morpholino]ethanesulfonic acid) buffer solution (pH around 6.4). A slight excess (5%) of ligand was used. The absence of free metal was checked through the xylenol orange test [32]. The $Gd(ClO_4)_3$ stock solution was made up by dissolving Gd_2O_3 in a slight excess of $HClO_4$ (Merck, p.a. 60%) in double-distilled water, followed by filtering. The pH of the stock solution was adjusted to 5.5 by addition of Gd_2O_3 and its concentration was determined by titration with Na_2H_2EDTA solution using xylenol orange as an indicator.

Sample preparation: For the critical micellar concentration determination a 17.02 mM $[Gd(EPTPA\text{-}C16)(H_2O)]^{2-}$ stock solution in 50 mM TRIS buffer was prepared. A series of $[Gd(EPTPA\text{-}C16)(H_2O)]^{2-}$ solutions with different concentrations were prepared by diluting

the stock solution. For the NMRD profiles two solutions were prepared from the 17.02 mM stock solution; one below (0.2 mM) and the other above (2mM) the CMC value previously determined. For the ^{17}O NMR measurements a 26.77 mmol kg^{-1} solution enriched to 2% using 10% ^{17}O-enriched water (Yeda R&D CO., Rehovot, Israel) was prepared.

Determination of the CMC by ^{1}H relaxivity measurements: The concentration range for this determination was 12.510-0.010 mM. For each sample, longitudinal ^{1}H relaxation rates were measured at 25ºC and 60MHz (1.41T) with a WP-60 electromagnet connected to a Bruker AC-200 console. The temperature was stabilized with a Bruker temperature control unit by gas flow. The longitudinal relaxation rate, $1/T_1$, was obtained with the inversion-recovery method.

NMRD measurements: The measurements were performed using a Stelar Spinmaster FFC NMR relaxometer (0.01-20 MHz) equipped with a VTC90 temperature control unit. The temperature was fixed by a gas flow. and a WP – electromagnet connected to a Bruker AC-200 console (0.47 – 1.41 T; 20-60 MHz). At higher fields, the ^{1}H relaxivity measurements were performed on Bruker Minispecs mq30 (30 MHz), mq40 (40 MHz) and mq60 (60 MHz) and on Bruker 50 MHz (1.18 T), 100 MHz (2.35 T) and 200 MHz (4.70 T) cryomagnets connected to a Bruker AC-200 console. In each case, the temperature was measured by a substitution technique. Longitudinal relaxation rates were measured at two different concentrations, one below (0.2 mM) and the other above the CMC (2mM) at 25ºC. Variable temperature measurements were performed at 5, 25 and 37ºC.

EPR

The spectra were recorded in a conventional Elexsys spectrometer E500 at X-band (9.4 GHz). A controlled nitrogen gas flow was used to maintain a constant temperature, which was measured by a substitution technique. The transverse electronic relaxation rates, $1/T_{2e}$, were calculated from the EPR line widths according to Reuben [36].

^{17}O NMR spectroscopy: The solution samples were sealed in glass spheres adapted for 10 mm NMR tubes to avoid susceptibility corrections of the chemical shift. Transverse and longitudinal ^{17}O relaxation rates and chemical shifts were measured for temperatures between -1.9ºC and 52ºC. Temperatures above 60ºC were not used to avoid compound decomposition. Data were recorded at two different magnetic fields (9.4 T, 4.7 T). Acidified water of pH 3.4 was used as an external reference.

Data analysis.

The least-squares fits on the ^{17}O NMR and NMRD relaxation data were performed with the Visualiseur/Optimiseur programs on a Matlab platform version 5.3 [33].

Materials and equipment: Chemicals were purchased from Sigma-Aldrich and used without further purification. Solvents used were of reagent grade and purified by usual methods. Reactions were monitored by TLC on Kieselgel 60 F_{254} (Merck) on aluminium support and on silica gel RP-18 on glass support (Fluka). Detection was by examination under UV light (254 nm), by adsorption of iodine vapour and spraying with ninhydrine. Flash chromatography was performed on Kieselgel 60 (Merck, mesh 230-400) and on silica gel 100C_8 – Reversed Phase (Fluka). The relevant fractions from flash chromatography were pooled and concentrated under reduced pressure, T<40 ^{o}C. ^{1}H and ^{13}C NMR spectra (assigned by 2D DQF-COSY and HMQC techniques) were run on a Varian Unity Plus 300 NMR spectrometer, operating at 299.938 MHz and 75.428 MHz, for ^{1}H and ^{13}C, respectively. Chemical shifts (δ) are given in ppm relative to the $CDCl_3$ solvent (^{1}H, δ 7.27; ^{13}C 77.36) as internal standard. For ^{1}H and ^{13}C NMR spectra recorded in D_2O, chemical shifts (δ) are given in ppm, respectively, relative to TSP as internal reference (^{1}H, δ 0.0) and *tert*-butanol as external reference (^{13}C, CH_3 δ 30.29). ^{13}C NMR spectra were proton broad-band decoupled using a decoupling scheme.

Synthesis and characterisation

Compound **2** (Garner's aldehyde) was synthesised by a three step procedure according to the literature [26].

Synthesis of fully protected triamine 4.

A solution of *NBoc*-1,3–propanediamine **3** (1.46 g, 8.37 mmol) and Garner aldehyde **2** (1.83 g, 7,98 mmol) in 1,2–dichloroethane (80 cm^3) was stirred at room temperature for 5 minutes before $NaBH(OAc)_3$ (1.72 g, 8,12 mmol) was added in small portions over 5 minutes. The clear solution became immediatelly cloudy and was left stirring over nitrogen for 2 hours. $NaHCO_3$ (saturated solution, 100 cm^3) was added, the organic phase was separated and the aqueous phase was extracted with dichloromethane (50 cm^3). The combined organic phase was washed with $NaHCO_3$ (2×80 cm^3) and brine (80 cm^3), dried ($MgSO_4$) and was concentrated under reduced pressure to give a crude yellow oil. Purification by flash column chromatography (15×2.5 cm, DCM → DCM/EtOH (3:1) yielded the title compound (2.54 g, 82%) as a colourless oil. ^{1}H NMR (300 MHz, $CDCl_3$): δ (ppm) = 1.44 (s, 9H, Boc); 1.48 (s, 9H, Boc); 1.54 (m, 6H, C(*CH*$_3$)$_2$); 1.63 (m, 2H, NHCH$_2$*CH*$_2$CH$_2$NHBoc); 2.65 (m, 1H, NHCHC*H*$_a$H$_b$NH) 2.71 (m, 2H, NH*CH*$_2$CH$_2$CH$_2$NHBoc); 2.88 (m, 1H, NHCHCH$_a$*H*$_b$NH); 3.19 (m, 2H, NHCH$_2$CH$_2$*CH*$_2$NHBoc); 3.78-3.40 (m, 3H, OC*H*$_a$*H*$_b$ and OCH$_2$C*H*); ^{13}C (56 MHz, D_2O): δ(ppm) = 23.06, 24.32, 26.77 and 27.56 (C(*C*H$_3$)$_2$), 28.40 (C(*C*H$_3$)$_3$); 29.68 (NHCH$_2$*C*H$_2$CH$_2$NHBoc); 39.26 (NHCH$_2$CH$_2$*C*H$_2$NHBoc), 47.72 (NH*C*H$_2$CH$_2$CH$_2$NHBoc); 51.48 (CH*C*H$_a$H$_b$NH); 57.04 and 57.19 (OCH$_2$*C*H); 66.21 (O*C*H$_2$); 78.93, 79.62 and 80.20 (*C*(CH$_3$)$_3$), 93.36 and 93.78 (*C*(CH$_3$)$_2$), 156.04 (NH*C*(O)O^{t}Bu); *HRMS* (FAB$^+$, NBA) *Calc. for* $C_{19}H_{38}N_3O_5$ $(M+H)^+$ 388.2811. *Found* 388.2815.

Synthesis of fully deprotected triamine 5: Compound **4** (2.32 g, 5.98 mmol) was stirred overnight at room temperature with aqueous HCl 6M/EtOH (1:1, 40 cm^3). The solvent was removed under reduced pressure. The residue was repeatedly co-evaporated with water, dissolved in water (~ 20 ml) and adjusted to pH 7 with DOWEX 1X-100-OH^- resin (~ 20 ml wet resin). The resin was filtered off and the filtrate was evaporated under reduced pressure to give a white vitreous solid (quantitative yield). This material was carried through without further purification. ^{1}H NMR (300 MHz, $CDCl_3$): δ (ppm) = 2.17 (qt, 2H, *J* = 7.5, $NHCH_2\mathit{CH_2}CH_2NH$); 3.14 (t, 2H, *J* = 7.5, $NH\mathit{CH_2}CH_2CH_2NH$); 3.21 (td, 2H, *J* = 7.5 and 2.4 Hz, $NH\mathit{CH_2}CH_2CH_2NH$); 3.30 (dd, 1H, *J* = 13.4 and 6.6, $NHCH(CH_2OH)C\mathit{H_a}H_bN$); 3.41 (dd, 1H, *J* = 13.4 and 5.4, $NHCH(CH_2OH)CH_a\mathit{H_b}N$), 3.72 (m, 1H, $NHC\mathit{H}(CH_2OH)CH_2N$), 3.87 (m, 2H, $NHCH(C\mathit{H_aH_b}OH)CH_2N$); MS ($EI^+$): *m/z* 148.15 $(M+H)^+$; *HRMS* (EI^+) *Calc. for* $C_6H_{18}N_3O(M+H)^+$ 148.1450. Found 148.1450.

Synthesis of fully alkylated compound 6

To compound **5** (3.12 g, 8.06 mmol), partially dissolved in DMF, was added DIPEA (11.0 cm^3, 64.5 mmol), tert-butylbromoacetate (9.0 cm^3, 60.5 mmol) and KI (1,63 g, 9.80 mmol). The solution became yellow and was left stirring over a period of 64 hours. The solvent was evaporated under reduced pressure giving rise to a yellow and a white solid. The residue was taken into ethyl acetate (200 cm^3) and the white solid was filtered off. The organic phase was washed with $NaHCO_3$ sat. sol. (2×100 cm^3), brine (100 cm^3) and dried ($MgSO_4$). The solvent was removed under reduced pressure giving rise to a yellow oil. Purification by flash chromatography (19×2.5cm) with Hexane → Hexane/Ethyl acetate (1:1) yielded the title compound (4.40 g, 76%) as a pale yellow oil. ^{1}H NMR (300 MHz, $CDCl_3$): δ (ppm) = 1.45 (s, 45H, $C(\mathit{CH_3})_3$); 1.60 (m, 2H, $NCH_2\mathit{CH_2}CH_2N$); 2.45-2.79 (m, 6H,

N*CH*(CH_aH_bOH)*CH_2*N*CH_2*CH_2*CH_2*N); 2.93 (m, 1H, N*CH*CH_2N); 3.211 (d, 1H, *J*= 6.9 Hz, NCH(C*H_a*H_bOH)CH_2N); 3.40 (s, 6H, acetate arms); 3.44 (s, 4H, acetate arms), 3.66 (1H, dd, *J* = 11.4 and 4.8 Hz, NCH(CH_a*H_b*OH)CH_2N); ^{13}C (56 MHz, $CDCl_3$): δ(ppm) = 26.20 (NCH$_2$*C*H$_2$CH$_2$N), 28.08 (C(*C*H$_3$)$_3$), 51.89 and 52.59 (N*C*H$_2$CH$_2$*C*H$_2$N), 53.59 (N*C*H$_2$C(O)O^{t}Bu), 54.32 (NCH*C*H$_2$N), 55.78 (N*C*H$_2$C(O)O^{t}Bu), 56.08 (N*C*H$_2$C(O)O^{t}Bu), 61.97 (N*C*H(CH_aH_bOH)CH_2N), 62.30 (NCH(*C*H_aH_bOH)CH_2N), 80.82, 80.95 and 81.07 (*C*(CH$_3$)$_3$), 17.59 and 171.83 (NCH$_2$*C*(O)O^{t}Bu), *HRM*S (FAB$^+$, NBA) *Calc. for* $C_{36}H_{68}N_3O_{11}$ $(M+H)^+$ 718.4845. Found 718.4854.

Synthesis of fully-deprotected palmitic ester conjugate 8

To a solution of compound **6** (1.68 g, 2.34 mmol) in anhydrous dichloromethane (30 cm^3) was added palmitic anhydride (2.29 g, 4.63 mmol), pyridine (1 cm^3, 12.5 mmol) and 4-dimethylaminopyridine (28.6 mg, 0.234 mmol) and the reaction mixture was stirred at room temperature under a nitrogen atmosphere. After 24 hours the reaction mixture was quenched with cold water. To the mixture was added dichloromethane (70 cm^3), the organic phase was separated and was washed with $KHSO_4$ (2×100 cm^3), $NaHCO_3$ (3×100 cm^3) and brine (1×100 cm^3), dried ($MgSO_4$) and concentrated under reduced pressure. The crude oil obtained was purified by flash chromatography (20×2.5 cm) with petroleum ether 40-60 → petroleum ether/ethyl acetate (1:1.5) to give the fully alkylated palmitic ester conjugate as an adduct with an extra molecule of palmitic acid **7**. ^{1}H NMR (300 MHz, $CDCl_3$) δ (ppm) = 0.89 (t, 6H, *CH_3*), 1.27 (m, 48H, *CH_2* alkyl chain), 1.46 (s, 45H, *t*Bu), 1.64 (m, 6H, overlapped signals from OC(O)CH$_2$C*H$_2$* and NCH$_2$*CH_2*CH$_2$N), 2.33 (m, 4H), 2.65 (m, 5H), 2.85 (dd, 1H, *J*= 13.5 and 5.4 Hz, NCH(CH$_2$O)CH$_a$*H$_b$*N), 3.11 (m, 1H, NC*H*), 3.28 (s, 2H, N*C*H$_2$C(O)O*t*Bu), 3.41 (s, 4H, N*C*H$_2$C(O)O*t*Bu), 3.49 (s, 4H, N*C*H$_2$C(O)O*t*Bu), 4.12-4.24

(m, 2H, NCHCH_aH_bO); *HRM*S (ESI$^+$) *Calc. for* $C_{52}H_{98}N_3O_{12}$ $(M+H)^+$ 956.7150. Found 956.7145. This material was carried through with out further purification.

The material **7** was stirred overnight at room temperature with DCM/TFA (3:1, 15 cm^3). The solvent was removed under reduced pressure, the residue was re-dissolved in DCM (20 cm^3) and the solvent was removed under reduced pressure. This procedure was repeated several times and the material was further dried under vacuum to give a white solid. To this material was added distilled water (100 cm^3) and the resulting suspension was adjusted to pH 7 with aqueous solution of KOH 0.1M. The suspension was filtrated through a nylon membrane filter (0.22 μm). The filtrate was concentrated under reduced pressure and the crude obtained was purified by flash chromatography on reversed phase RP_8 silica with gradient elution 100% H_2O → 100% EtOH. The relevant fractions were pooled and the solvent was removed under reduced pressure to afford the title compound as a white solid (0.76 g, 48% over two steps). ^{1}H NMR (300 MHz, D_2O): δ (ppm) = 0.87 (t, 3H, *CH*$_3$), 1.28 (m, 24H, *CH*$_2$ alkyl chain), 1.60 (m, 2H, OC(O)CH_2C*H*$_2$), 2.09 (m, 2H, NCH_2*CH*$_2$$CH_2$N), 2.43 (t, 2H, *J* = 7.2 Hz, OC(O)*CH*$_2$), 3.0-3.40 (m, 6H, overlapping signals from NCH(CH_2OH)*CH*$_a$*H*$_b$N*CH*$_2$$CH_2$*CH*$_2$N), 3.51 (s, 4H, acetate protons), 3.62 (m, 3 H overlapping signals from N*CH*(CH_2OH)CH_2N and central acetate protons), 3.77 (s, 4H, acetate protons), 4.26 (m, 2H, NCH(*CH*$_2$O)CH_2N); ^{13}C (56 MHz, D_2O): δ (ppm) = 16.68 (*C*H_3, alkyl chain), 23.70 (NCH_2*C*$H_2$$CH_2$N), 25.35 (*C*$H_2$ alkyl chain), 27.27 (OC(O)CH_2*C*H_2), 31.58, 31.82, 32.01, 32.08, 32.23, 32.30, 32.33 and 34.59 (*C*H_2 alkyl chain), 36.63 (OC(O)*C*H_2), 45.88, 53.98 (NCH(CH_2OH)*C*H_2N), 56.22 and 56.50 (N*CH*$_2$$CH_2$*CH*$_2$N), 57.41 and 57.33-57.64 (cluster of signals from N*C*H_2COOH), 59.92 (N*C*H(CH_2OC(O))CH_2N), 60.10 (N*C*H_2COOH), 64.18 (NCH(*C*H_2OC(O))CH_2N), 174.00 (C(O), ester), 176.16, 178.57 and 178.98 (C(O), carboxylic acid). MS (ESI$^+$): *HRM*S (ESI) *Calc. for* $C_{32}H_{58}N_3O_{12}$ $(M+H)^+$ 676.4001. Found 676.4015.

Acknowledgments

This work was performed within the framework of the EU COST Action D18 "Lanthanide chemistry for diagnosis and therapy". The work was supported by the Foundation of Science and Technology (F.C.T.), Portugal (project POCTI/QUI/47005/2002) and FEDER. É. Tóth acknowledges the Swiss National Science Foundation and the Swiss Federal Office for Education and Science for financial support.

Supporting Information:

Table 1S: Transverse relaxation rate enhancement for $[Gd(EPTPA\text{-}C16)(H_2O)]^{2-}$ solutions with different Gd(III) concentrations.

Table 2S: Proton relaxivities for a 0.2 mM $[Gd(EPTPA\text{-}C16)(H_2O)]^{2-}$ solution (non aggregated form).

Table 3S: Proton relaxivities in 2 mM $[Gd(EPTPA\text{-}C16)(H_2O)]^{2-}$ (aggregated form).

Table 4S: Proton relaxivities resulting from the micellar form calculated using the equation $r_1^a = \left(R_1^{obs} - R_1^d - r_1^{n.a.} \times cmc\right)/\left(c_{Gd} - cmc\right)$.

Table 5S: Variable temperature reduced transverse and longitudinal ^{17}O relaxation rates and chemical shifts of $[Gd(EPTPA\text{-}C16)(H_2O)]^{2-}$ solution at 9.4 T. c_{Gd} = 26,77mmol/Kg; P_m = 4.81×10^{-4}

Table 6S: Variable temperature reduced transverse and longitudinal ^{17}O relaxation rates and chemical shifts of $[Gd(EPTPA\text{-}C16)(H_2O)]^{2-}$ solution at 4.7T. c_{Gd} = 26.77 mmol/kg; P_m = 4.81×10^{-4}.

References

1. R. B. Lauffer, *Chem. Rev*., 87 (1987) 901-927.

2. S. Aime, M. Botta, M. Fasano, E. Terreno, *Chem. Soc. Rev*., 27 (1998) 19-29.

3. V. Comblin, D. Gilsoul, M. Hermann, V. Humbert, V. Jacques, M. Mesbari, C. Sauvage, J. F. Desreux, *Coord. Chem. Rev*., 185-186 (1999) 451-470.

4. P. Caravan, J. J. Ellison, T. J. McMurry, R. B. Lauffer, *Chem. Rev*., 99 (1999) 2293-23525.

5. M. P. Lowe, *Austr. J. Chem*., 55 (2002) 551-556.

6. É. Tóth, L. Helm, A. E. Merbach, *Top. Current Chem*., 221 (2002) 61-101.

7. É. Tóth, L. Helm, A.E. Merbach "Relaxivity of Gadolinium(III) Complexes: Theory and Mechanism" in *The Chemistry of Contrast Agents in Medical Magnetic Resonance Imaging*, (Eds. A. E. Merbach, É. Tóth) John Wiley & Sons Wiley, Chichester, 2001, p. 45-119.

8. A. D. Nunn, K. E. Linder, M. F. Tweedle, *Q. J. Nucl. Med*., 41 (1997) 155.

9. S. Aime, C. Cabella, S. Colombato, S. G. Crich, E. Gianolio, F. Maggiori, *J. Magn. Res.* 16 (2002) 394-406.

10. E. Tóth, D. Pubanz, S. Vanthey, L. Helm, A. E. Merbach, *Chem. Eur. J.,* 2 (1996) 1607-1615.

11. S. Aime, M. Botta, M. Fasano, E. Terreno, "Protein-bound metal chelates" in *The Chemistry of Contrast Agents in Medical Magnetic Resonance Imaging*, (Eds. A. E. Merbach, E. Tóth) John Wiley & Sons, Chichester, 2001, p.193.

12. a) J. P. André, C. F. G. C. Geraldes, J. A. Martins, A. E. Merbach, M. I.M. Prata, A.C. Santos, J.J. P. de Lima, É. Tóth, *Chem. Eur. J.*, 10 (2004) 5804-5816; b) P. Baía, J. P. André, C. F. G. C. Geraldes, J. A. Martins, A. E. Merbach, , É. Tóth,. *Eur. J. lnor. Chem*, (in press).

13. J. P. André, É. Tóth, H. Fischer, A. Seelig, H. R. Mäcke, A. E. Merbach, *Chem. Eur. J.*, 5 (1999) 2977-2983.

14. V. P. Torchilin, *Adv. Drug Delivery*, 54 (2002) 235-252.

15. S. M. Moghini, A. C. Hunter, J. C. Murray, *Pharm. Rev.* 53 (2001) 283-318.

16. K. Kostarelos, D. Emfietzoglon, *J. Liposome* 9 (1999) 429-460.

17. V. P. Torchilin, M. D. F. Kamenetsky, G. L. Wolff, *Acad. Radiol.* 6 (1999) 61-65.

18. B. Goins, W. T. Phillips, R. Klipper, *J. Nucl. Med.* 37 (1996) 1374-1379.

19. W. T. Phillips, R. Klipper, B. Goins, *J. Pharm. and Exper. Therapeutics*, 295 (2000) 309-313.

20. G. M. Nicolle, L. Helm, A. Merbach, *Magn. Reson. Chem*., 41 (2003) 794-799.

21. G. M. Nicolle, É. Tóth, K.-P. Eisenwiener, H. R. Mäcke, A. E. Merbach, *J. Biol. Inorg. Chem.*, 7 (2002) 757-769.

22. R. Ruloff, É. Tóth, R. Scopelliti, R. Tripier, H. Handel, A. E. Merbach, *Chem. Comm.*, (2002) 2630-2631

23 a) T.-H. Cheng, Y.-M. Wang, K.-T. Lin, G.-C. Liu, *Dalton Trans*. **2001**, 3357-3366; b) S. Laus, R. Ruloff, É. Tóth, A. E. Merbach, *Chem. Eur. J.*, 9 (2003) 3555-3566.

24. A. Congreve, D. Parker, E. Gianolio, M. Botta, *Dalton Trans*., (2004) 1441-1445.

25. S. Laus, A. Sour, R. Ruloff, É. Tóth, A. E. Merbach, *Chem. Eur. J.,* 11 (2005) 3064-3076.

26. a) P. Meffre, P. Durand, E. Branquet, F. Le Goffic, *Synth. Commun.*, 24, 2147-2152, 1994; b) E. Branquet, P. Durand, Vo-Quang, F. Le Goffic, *Synth. Commun,* 23, 153-156, 1993, c) P. Garner, *Tetrahedron Lett*., 25, 5855-5858, 1984.

27. A.F. Abdel-Magid, K.G. Carson, B.D. Harris, C.A. Maryanoff, R.D. Shah, *J. Org. Chem.*, 61, 3849-3862, 1996.

28. G. Lipari, A. Szabo, *J. Am. Chem. Soc*., 104 (1982) 4546-4558.

29. G. Lipari, A. Szabo, *J. Am. Chem. Soc*., 104 (1982) 4559-4570.

30. F. Dunand, A. Borel, A. E. Merbach, *J. Am. Chem. Soc.,* 124*,* (2002) 710-716.

31. F. Yerly, K. I. Hardcastle, L. Helm, S. Aime, M. Botta, A. E. Merbach, *Chem. Eur. J.,* 8 (2002) 1031-1039.

32. G. Brunisholz, M. Randin, *Helv. Chim. Acta*, 42 (1959) 1927-1938.

33. F. Yerly, VISUALISEUR 2.3.4, and OPTIMISEUR 2.3.4, Lausanne (Switzerland), 1999.

34. G. M. Nicolle, É. Tóth, H. S.-Willich, B. Radüchel, A. E. Merbach, *Chem. Eur. J*., 5 (2002) 1040-1048.

35. G.M. Nicolle, É. Tóth, K.P. Eisenwiener, H.R. Mäcke, A.E. Merbach, J. *Biol. Inorg. Chem*., 7 (2002) 757-769.

36. J. Reuben, *J. Phys. Chem.*, 75 **(**1971) 3164.

Table 1. Parameters obtained from the simultaneous fit of ^{17}O NMR, EPR and ^{1}H NMRD data for the aggregated form of the $[GdEPTPAC16(H_2O)]^{2-}$ complex.

Parameter	
k_{ex}^{298} / $10^6 s^{-1}$	170±30
$\Delta H^{\ddagger}$ / kJmol^{-1}	23.6±1.0
τ_g^{298} / ps	2100±200
E_g / kJmol^{-1}	19.3±1.0
τ_l / ps	330±40
E_l / kJmol^{-1}	49.0±2.0
S^2	0.41±0.08

Table 2 – Relaxivity (at 20 MHz and 25 °C) and parameters determining relaxivity for selected Gd^{III} complexes.

	k_{ex}^{298} / ($\times 10^6$ s^{-1})	τ_{gO} (ps)	τ_{lO} (ps)	S^2	r_1 ($mM^{-1}s^{-1}$)
Small molecular weight chelates					
[Gd(EPTPA-bz-NO_2)(H_2O)] $^{2-}$ [23]	150	τ_{RO} = 122	–	-	4.73
[Gd(EPTPA)(H_2O)]$^{2-}$ [23]	330	τ_{RO} = 75	–	-	
[Gd(TRITA)(H_2O)]$^-$ [22]	270	τ_{RO} = 82	–	-	
[Gd(EPTPA-C16)(H_2O)]$^{2-}$ [a, b]	170	τ_{RH} = 200	–	-	9.11
Dendrimers					
Gadomer 17 [34]	1.0	3050	760	0.50	16.46
G5-(GdEPTPA)$_{115}$ [25]	150	4040	150	0.43	23.9 [c]
Micelles					
[Gd(DOTASAC12(H_2O)]$^-$ [13]	4.8	920	-	-	18.03
[Gd(DOTAC10)(H_2O)]$^-$ [35]	4.8	τ_{RO} = 470	-	-	9.32
[Gd(DOTAC12)(H_2O)]$^-$ [35]	4.8	1600	430	0.23	17.24
[Gd(DOTAC14)(H_2O)]$^-$ [35]	4.8	2220	820	0.17	21.45
[Gd(DOTASAC18)(H_2O)]$^-$ [35]	4.8	2810	330	0.28	20.72
[Gd(EPTPAC16)(H_2O)]$^-$ [a]	170	2100	330	0.41	22.59

[a] This work
[b] non-aggregated form
[c] 37 °C

Scheme 1. Synthetic route for the synthesis of hydroxymethy(EPTA) palmitoyl ester conjugate. a) $NaBH(OAc)_3$/1,2-dichloroethane; b) i) HCl (aq. sol. 6M)/EtOH (1/1), ii) titration to pH 7 with Dowex1-X2-100-OH^-; c) *t*Bu-bromoacetate, DIPEA, KI/DMF; d) palmitic anhydride, Py, DMAP/CH_2Cl_2; e) i) TFA/CH_2Cl_2 (3/1), ii) titration to pH 7.0 with aq. KOH, iii) RPC_8 flash chromatography.

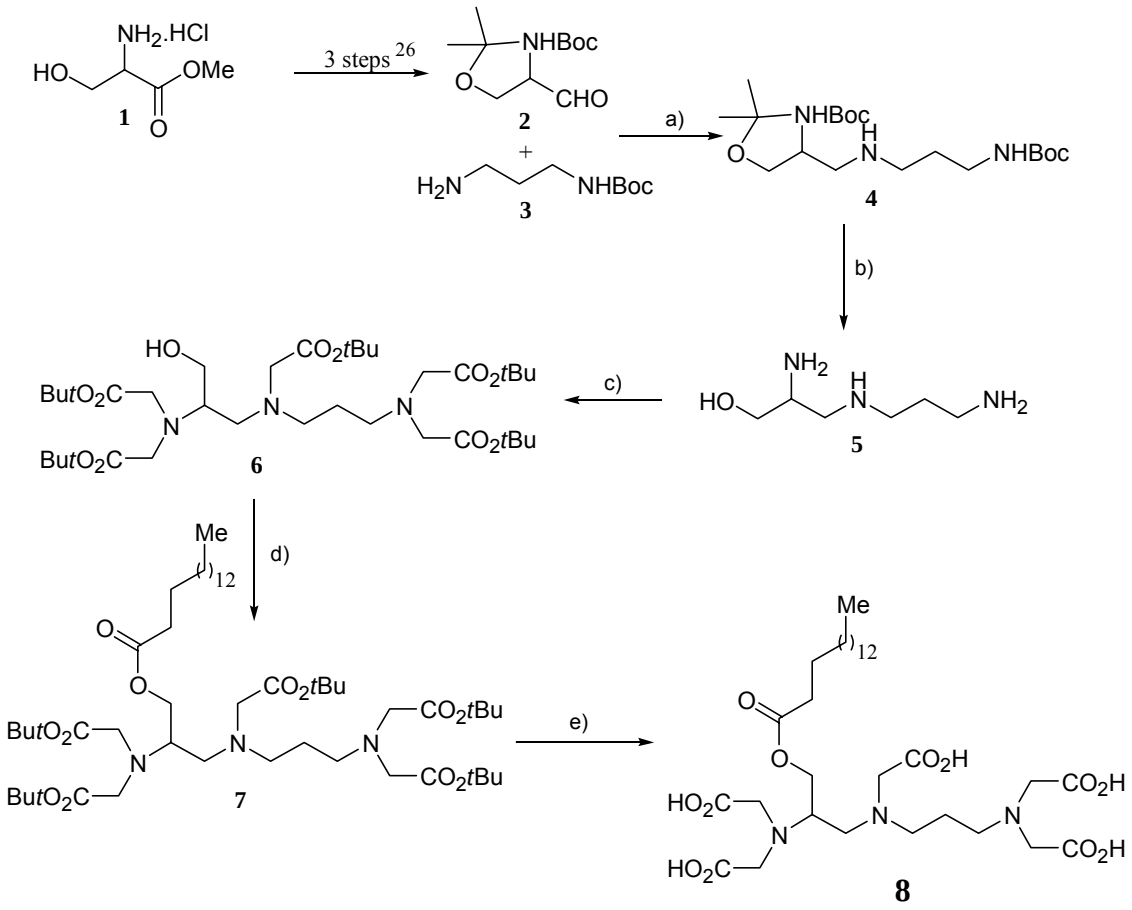

Scheme 1

Figure Legends

Figure 1 - Variation of the water ^{1}H longitudinal relaxation rate versus the total Gd^{III} concentration at 60MHz and 25ºC for $[Gd(EPTPA\text{-}C16)(H_2O)]^{2-}$, and least-squares fit according to Equation (2).

Figure 2 - The CMC obtained for $[Gd(EPTPA\text{-}C16)(H_2O)]^{2-}$ is in accordance with the values for previously reported systems.

Figure 3 - ^{1}H nuclear magnetic relaxation dispersion profiles of the monomer form of $[Gd(EPTPA\text{-}C16)(H_2O)]^{2-}$ (0.2 mM). 5°C (○), 25 °C (□) and 37 °C (▽).

Figure 4 – Temperature dependence of **(a)** reduced transverse and longitudinal ^{17}O relaxation rates $1/T_{2r}$ and $1/T_{1r}$, respectively; B = 9.4 T ($\ln(1/T_{1r})$: □, ($\ln(1/T_{2r})$: ○ and B = 4.7 T ($\ln(1/T_{1r})$: ▽, ($\ln(1/T_{2r})$: +; **(b)** reduced chemical shifts $\Delta\omega_r$ (B = 9.4 T: □ and B = 4.7 T: ▽) of $[Gd(EPTPA\text{-}C16)(H_2O)]^{2-}$ (c_{Gd} = 26.77 $mmolkg^{-1}$). **(c)** ^{1}H nuclear magnetic relaxation dispersion profiles of the aggregated form (2 mM), recorded at 5 ºC (○), 25 ºC (□), 37 ºC (▽). The lines represent the least-squares fit of the data points as explained in the text.

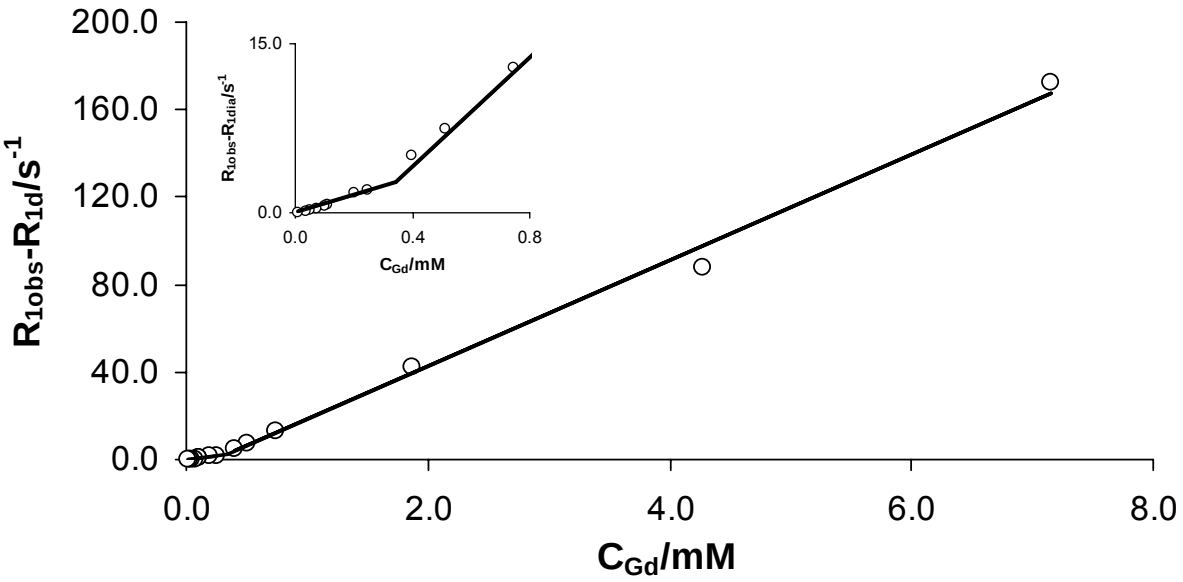

Figure 1 - Variation of the water ^{1}H longitudinal relaxation rate versus the total Gd^{III} concentration at 60MHz and 25ºC for $[Gd(EPTPA\text{-}C16)(H_2O)]^{2-}$, and least-squares fit according to Equation (2).

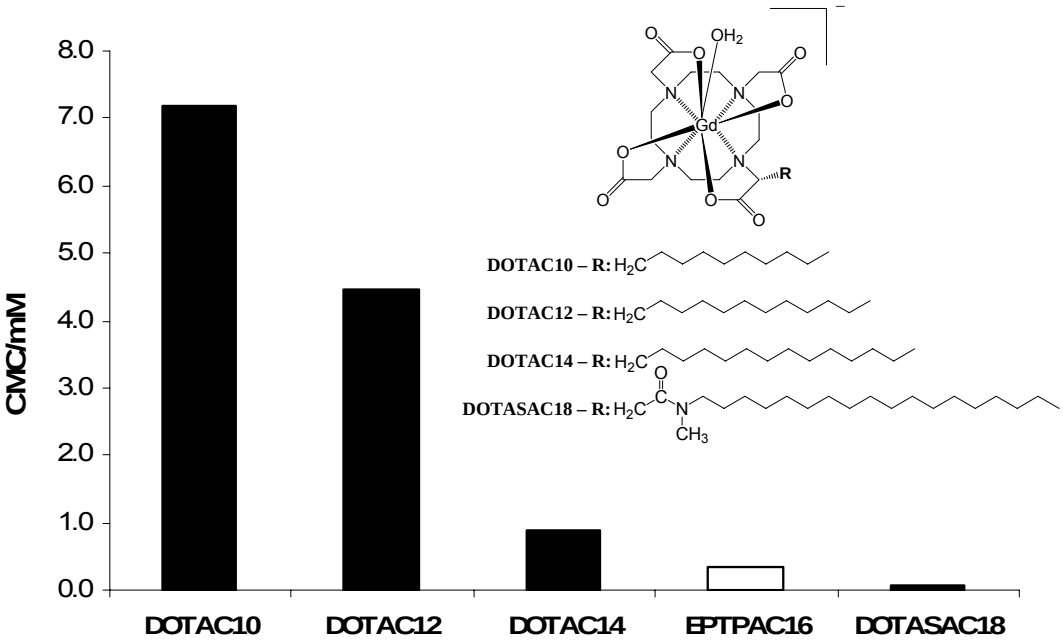

Figure 2 - The CMC obtained for $[Gd(EPTPA\text{-}C16)(H_2O)]^{2-}$ is in accordance with the values for previously reported systems.[35]

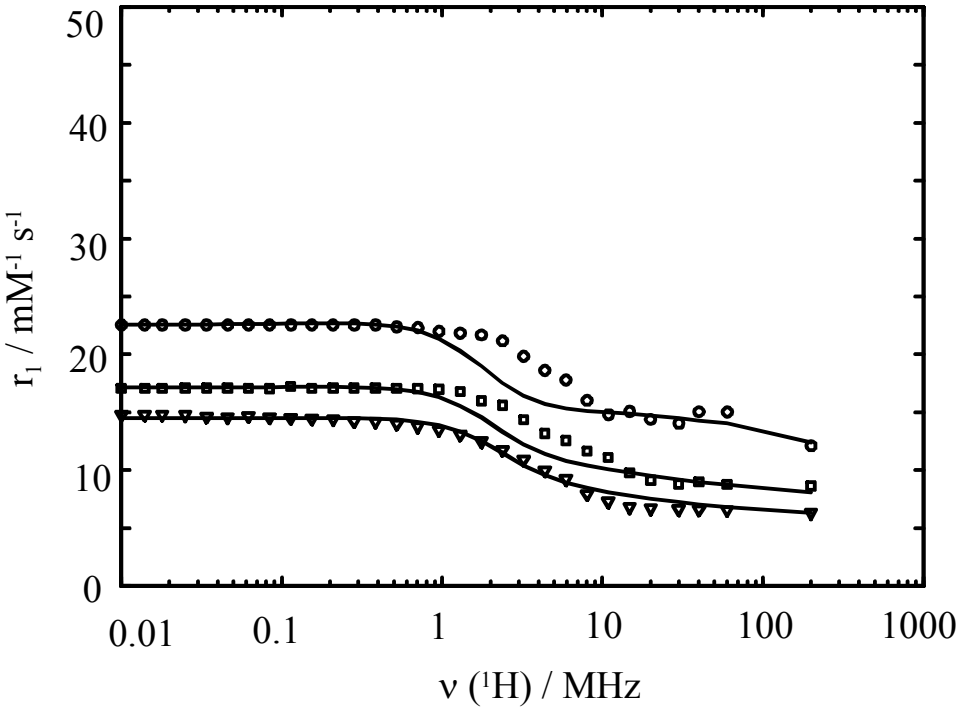

Figure 3 - ^{1}H nuclear magnetic relaxation dispersion profiles of the monomer form of $[Gd(EPTPA\text{-}C16)(H_2O)]^{2-}$ (0.2 mM). 5°C (○), 25 °C (□) and 37 °C (▽).

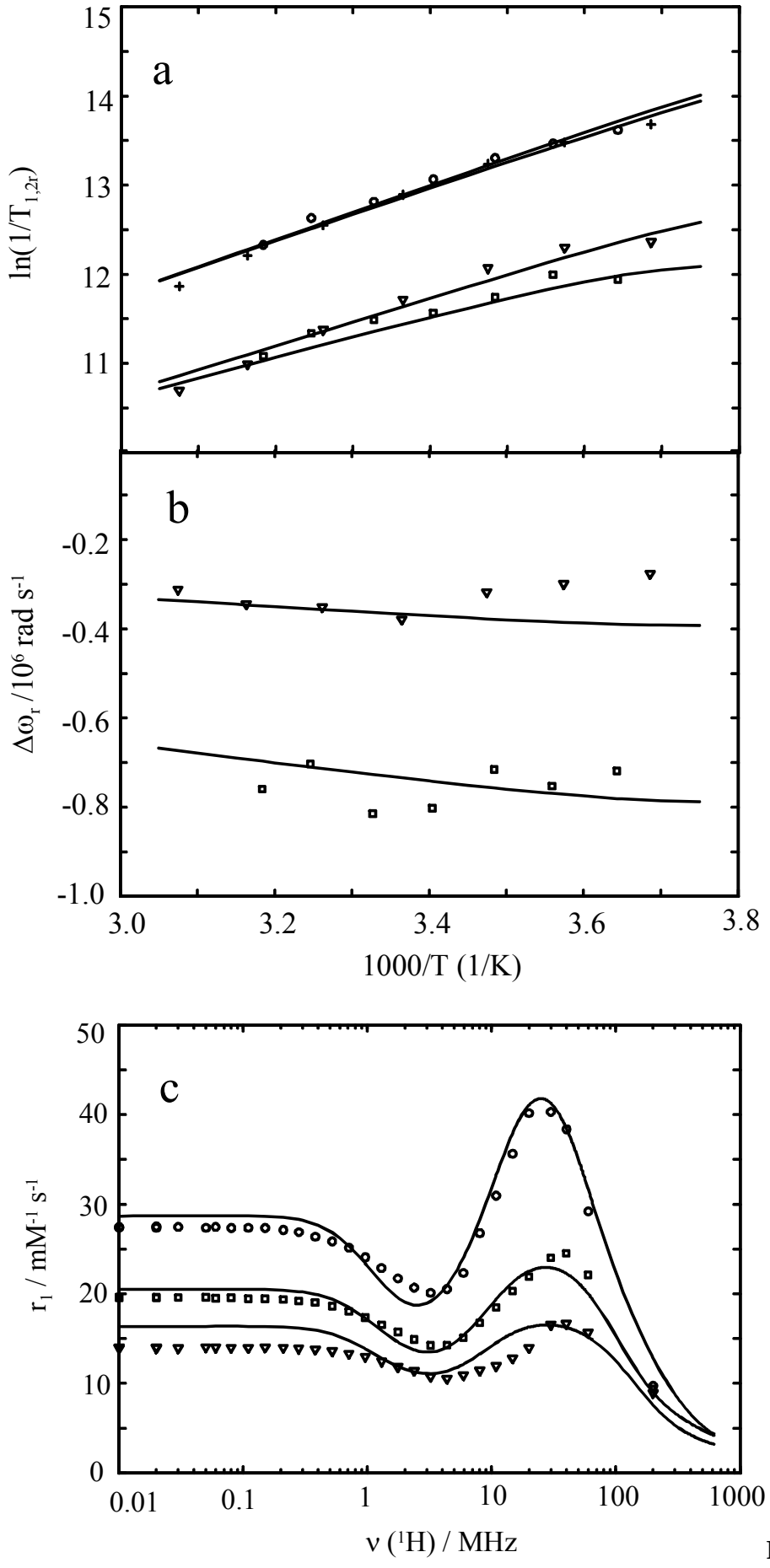

Fig. 4

Figure 4 – Temperature dependence of **(a)** reduced transverse and longitudinal ^{17}O relaxation rates $1/T_{2r}$ and $1/T_{1r}$, respectively; B = 9.4 T ($\ln(1/T_{1r})$: □, ($\ln(1/T_{2r})$: ○ and B = 4.7 T ($\ln(1/T_{1r})$: ▽, ($\ln(1/T_{2r})$: +; **(b)** reduced chemical shifts $\Delta\omega_r$ (B = 9.4 T: □ and B = 4.7 T: ▽) of $[Gd(EPTPA\text{-}C16)(H_2O)]^{2-}$ (c_{Gd} = 26.77 mmolkg^{-1}). **(c)** ^1H nuclear magnetic relaxation dispersion profiles of the aggregated form (2 mM), recorded at 5 ºC (○), 25 ºC (□), 37 ºC (▽). The lines represent the least-squares fit of the data points as explained in the text.

Supporting information

Equations used for the analysis of NMRD, EPR and ^{17}O NMR data.

^{17}O NMR spectroscopy

From the measured ^{17}O NMR relaxation rates and angular frequencies of the paramagnetic solutions, $1/T_1$, $1/T_2$ and ω, and of the acidified water reference, $1/T_{1A}$, $1/T_{2A}$ and ω_A, one can calculate the reduced relaxation rates and chemical shift, $1/T_{1r}$, $1/T_{2r}$ and $\Delta\omega_r$ (Eq. 1-3), where $1/T_{1m}$, $1/T_{2m}$ are the relaxation rates of the bound water and $\Delta\omega_m$ is the chemical shift difference between bound and bulk water, τ_m is the mean residence time or the inverse of the water exchange rate k_{ex} and P_m is the mole fraction of the bound water.[1,2]

$$\frac{1}{T_{1r}} = \frac{1}{P_m}\left[\frac{1}{T_1} - \frac{1}{T_{1A}}\right] = \frac{1}{T_{1m} + \tau_m} + \frac{1}{T_{1os}} \qquad \textbf{(1)}$$

$$\frac{1}{T_{2r}} = \frac{1}{P_m}\left[\frac{1}{T_2} - \frac{1}{T_{2A}}\right] = \frac{1}{\tau_m}\frac{T_{2m}^{-2} + \tau_m^{-1}T_{2m}^{-1} + \Delta\omega_m^2}{(\tau_m^{-1} + T_{2m}^{-1})^2 + \Delta\omega_m^2} + \frac{1}{T_{2os}} \qquad \textbf{(2)}$$

$$\Delta\omega_r = \frac{1}{P_m}(\omega - \omega_A) = \frac{\Delta\omega_m}{(1 + \tau_m T_{2m}^{-1})^2 + \tau_m^2\Delta\omega_m^2} + \Delta\omega_{os} \qquad \textbf{(3)}$$

Previous studies have shown that outer sphere contributions to the ^{17}O relaxation rates are negligible.[3] Eqs. 1 and 2 can be further simplified:

$$\frac{1}{T_{1r}} = \frac{1}{T_{1m} + \tau_m} \qquad \textbf{(4)}$$

$$\frac{1}{T_{2r}} = \frac{1}{T_{2m} + \tau_m} \qquad \textbf{(5)}$$

The exchange rate is supposed to assume the Eyring equation. In Eq. 6 $\Delta S^{\ddagger}$ and $\Delta H^{\ddagger}$ are the entropy and enthalpy of activation for the water exchange process, and k_{ex}^{298} is the exchange rate at 298.15 K.

$$\frac{1}{\tau_m} = k_{ex} = \frac{k_B T}{h} exp\left\{\frac{\Delta S^{\ddagger}}{R} - \frac{\Delta H^{\ddagger}}{RT}\right\} = \frac{k_{ex}^{298} T}{298.15} exp\left\{\frac{\Delta H^{\ddagger}}{R}\left(\frac{1}{298.15} - \frac{1}{T}\right)\right\} \qquad \textbf{(6)}$$

In the transverse relaxation the scalar contribution, $1/T_{2sc}$, is the most important [Eq. 7]. $1/\tau_{s1}$ is the sum of the exchange rate constant and the electron spin relaxation rate.

$$\frac{1}{T_{2m}} \cong \frac{1}{T_{2sc}} = \frac{S(S+1)}{3}\left(\frac{A}{\hbar}\right)^2 \tau_{s1} \qquad \textbf{(7)}$$

$$\frac{1}{\tau_{s1}} = \frac{1}{\tau_m} + \frac{1}{T_{1e}}$$

The ^{17}O longitudinal relaxation rates in Gd(III) solutions are the sum of the contributions of the dipole-dipole and quadrupolar (in the approximation developed by Halle) mechanisms as expressed by Eq. 10-12 for non-extreme narrowing conditions, where γ_S is the electron and γ_I is the nuclear gyromagnetic ratio ($\gamma_S = 1.76\times10^{11}$ rad s^{-1} T^{-1}, $\gamma_I = -3.626\times10^7$ rad s^{-1} T^{-1}), r_{GdO} is the effective distance between the electron charge and the ^{17}O nucleus, I is the nuclear spin (5/2 for ^{17}O), χ is the quadrupolar coupling constant and η is an asymmetry parameter :

$$\frac{1}{T_{1m}} = \frac{1}{T_{1dd}} + \frac{1}{T_{1q}} \qquad \textbf{(8)}$$

with:

$$\frac{1}{T_{1dd}} = \frac{2}{15}\left(\frac{\mu_0}{4\pi}\right)^2 \frac{\hbar^2\gamma_I^2\gamma_S^2}{r_{GdO}^6} S(S+1)\times\left[3J(\omega_I;\tau_{d1}) + 7J(\omega_S;\tau_{d2})\right] \qquad \textbf{(9)}$$

$$\frac{1}{T_{1q}} = \frac{3\pi^2}{10}\frac{2I+3}{I^2(2I-1)}\chi^2(1+\eta^2/3)\times\left[0.2J_1(\omega_I) + 0.8J_2(\omega_I)\right] \qquad \textbf{(10)}$$

In Eq. 3, the chemical shift of the bound water molecule, $\Delta\omega_m$, depends on the hyperfine interaction between the Gd(III) electron spin and the ^{17}O nucleus and is directly proportional to the scalar coupling constant, $\frac{A}{\hbar}$, as expressed in Eq. 11.[4]

$$\Delta\omega_m = \frac{g_L\mu_B S(S+1)B}{3k_B T}\frac{A}{\hbar} \qquad \textbf{(11)}$$

The isotopic Landé g factor is equal to 2.0 for the Gd(III), B represents the magnetic field, and k_B is the Boltzmann constant.

The outer sphere term of the chemical shift was found proportional to $\Delta\omega_m$, through an empirical constant C_{os}.[5]

$$\Delta\omega_{os} = C_{os}\Delta\omega_m \qquad \textbf{(12)}$$

For slowly rotating species, the spectral density functions are described the Lipari-Szabo approach.[6,7] In this model we distinguish two statistically independent motions; a rapid local motion with a correlation time τ_l and a slower global motion with a correlation time τ_g.

Supposing the global molecular reorientation is isotropic, the relevant spectral density functions are expressed as in Eq. 13-16, where the general order parameter S^2 describes the degree of spatial restriction of the local motion. If the local motion is isotropic, $S^2 = 0$; if the rotational dynamics is only governed by the global motion, $S^2 = 1$.

$$J(\omega_I;\tau_{d1}) = \left(\frac{S^2\tau_{d1g}}{1+\omega_I^2\tau_{d1g}^2} + \frac{(1-S^2)\tau_{d1}}{1+\omega_I^2\tau_{d1}^2} \right) \quad \textbf{(13)}$$

$$J(\omega_S;\tau_{d2}) = \left(\frac{S^2\tau_{d2g}}{1+\omega_S^2\tau_{d2g}^2} + \frac{(1-S^2)\tau_{d2}}{1+\omega_S^2\tau_{d2}^2} \right) \quad \textbf{(14)}$$

$$\frac{1}{\tau_{dig}} = \frac{1}{\tau_m} + \frac{1}{\tau_g} + \frac{1}{T_{ie}} \qquad i = 1, 2 \quad \textbf{(15)}$$

$$\frac{1}{\tau} = \frac{1}{\tau_g} + \frac{1}{\tau_l} \quad \textbf{(16)}$$

$$J_i(\omega_I) = \left(\frac{S^2\tau_g}{1+i^2\omega_I^2\tau_g^2} + \frac{(1-S^2)\tau}{1+i^2\omega_I^2\tau^2} \right) \qquad i = 1, 2 \quad \textbf{(17)}$$

^{1}H-NMRD

The measured longitudinal proton relaxation rate, R_1^{obs} is the sum of a paramagnetic and a diamagnetic contribution as expressed in Eq. 18, where r_1 is the proton relaxivity:

$$R_1^{obs} = R_1^d + R_1^p = R_1^d + r_1\,[Gd^{3+}] \quad \textbf{(18)}$$

The relaxivity can be divided into an inner and an outer sphere term as follows:

$$r_1 = r_{1is} + r_{1os} \quad \textbf{(19)}$$

The inner sphere term is given in Eq. 20, where q is the number of inner sphere water molecules [8].

$$r_{1is} = \frac{1}{1000} \times \frac{q}{55.55} \times \frac{1}{T_{1m}^H + \tau_m} \quad \textbf{(20)}$$

The longitudinal relaxation rate of inner sphere protons, $1/T_{1m}^H$ is expressed by Eq. 21, where r_{GdH} is the effective distance between the electron charge and the ^{1}H nucleus, ω_I is the proton resonance frequency and ω_S is the Larmor frequency of the Gd(III) electron spin.

$$\frac{1}{T_{1m}^{H}} = \frac{2}{15}\left(\frac{\mu_0}{4\pi}\right)^2 \frac{\hbar^2\gamma_I^2\gamma_S^2}{r_{GdH}^6} S(S+1) \times \left[3J(\omega_I;\tau_{d1}) + 7J(\omega_S;\tau_{d2})\right] \quad \textbf{(21)}$$

$$\frac{1}{\tau_{di}} = \frac{1}{\tau_m} + \frac{1}{\tau} + \frac{1}{T_{ie}} \quad \textbf{(22)}$$

The spectral density functions are given by Eq. 13-15.

The longitudinal and transverse electronic relaxation rates, $1/T_{1e}$ and $1/T_{2e}$ are expressed by Eq. 23-24, where τ_V is the electronic correlation time for the modulation of the zero-field-splitting interaction, E_V the corresponding activation energy and Δ^2 is the mean square zero-field-splitting energy. We assumed a simple exponential dependence of τ_V versus $1/T$ as written in Eq. 29.

$$\left(\frac{1}{T_{1e}}\right)^{ZFS} = \frac{1}{25}\Delta^2\tau_v\left\{4S(S+1) - 3\right\}\left(\frac{1}{1+\omega_S^2\tau_v^2} + \frac{4}{1+4\omega_S^2\tau_v^2}\right) \quad \textbf{(23)}$$

$$\left(\frac{1}{T_{2e}}\right)^{ZFS} = \Delta^2\tau_v\left(\frac{5.26}{1+0.372\omega_S^2\tau_v^2} + \frac{7.18}{1+1.24\omega_S\tau_v}\right) \quad \textbf{(24)}$$

$$\tau_v = \tau_v^{298}\, exp\left\{\frac{E_v}{R}\left(\frac{1}{T} - \frac{1}{298.15}\right)\right\} \quad \textbf{(25)}$$

The outer-sphere contribution can be described by Eq. 26 where N_A is the Avogadro constant, and J_{os} is its associated spectral density function [9,10].

$$r_{1os} = \frac{32N_A\pi}{405}\left(\frac{\mu_0}{4\pi}\right)^2 \frac{\hbar^2\gamma_S^2\gamma_I^2}{a_{GdH}D_{GdH}} S(S+1)\left[3J_{os}(\omega_I, T_{1e}) + 7J_{os}(\omega_S, T_{2e})\right] \quad \textbf{(26)}$$

$$J_{os}(\omega, T_{je}) = Re\left[\frac{1 + 1/4\left(i\omega\tau_{GdH} + \frac{\tau_{GdH}}{T_{je}}\right)^{1/2}}{1 + \left(i\omega\tau_{GdH} + \frac{\tau_{GdH}}{T_{je}}\right)^{1/2} + 4/9\left(i\omega\tau_{GdH} + \frac{\tau_{GdH}}{T_{je}}\right) + 1/9\left(i\omega\tau_{GdH} + \frac{\tau_{GdH}}{T_{je}}\right)^{3/2}}\right] \quad \textbf{(27)}$$

$j = 1, 2$

The diffusion coefficient for the diffusion of a water proton away from a Gd(III) complex, D_{GdH}, is assumed to obey an exponential law versus the inverse of the temperature, with an activation energy $E_{GdH,}$ as given in Eq. 28. D_{GdH}^{298} is the diffusion coefficient at 298.15K.

$$D_{\mathrm{GdH}} = D_{\mathrm{GdH}}^{298} \exp\left\{\frac{E_{\mathrm{GdH}}}{R}\left(\frac{1}{298.15} - \frac{1}{T}\right)\right\} \qquad \textbf{(28)}$$

References for Equations.

[1] T. J. Swift, R. E.Connick, *J. Chem. Phys.*, **1962**, *37*, 307-320.

[2] J. R. Zimmermann, W. E. Brittain, *J. Phys. Chem.*, **1957**, *61*, 1328-1333.

[3] K. Micskei, L. Helm, E. Brücher, A. E. Merbach, *Inorg. Chem.,* **1993**, *32*, 3844-3850.

[4] H. G. Brittain, J. F. Desreux, *Inorg. Chem*., **1984**, *23*, 4459-4466.

[5] G. Gonzalez, H. D. Powell, V. Tissières, A. E. Merbach, *J. Phys. Chem.*, **1994**, *98*, 53-59.

[6] G. Lipari, S. Szabo, *J. Am. Chem. Soc.*, **1982**, *104*, 4546-4559.

[7] G. Lipari, S. Szabo, *J. Am. Chem. Soc.*, **1982**, *104*, 4559-4570.

[8] Z. Luz, S. Meiboom, *J. Chem. Phys.*, **1964**, *40*, 2686.

[9] J. H. Freed, *J. Chem. Phys*., **1978**, *68*, 4034-4037.

[10] S.H. Koenig, R. D. Brown III, *Prog. Nucl. Magn Reson. Spectrosc.*, **1991**, *22*, 487-567.

Table 1S: Longitudinal water proton relaxation rate enhancement for [Gd(EPTPA-C16)(H_2O)]$^{2-}$ solutions with different Gd^{III} concentrations. ([a] the diamagnetic contribution to the longitudinal relaxation rate results from a 50 mM TRIS buffer solution).

$[Gd^{3+}]$/mM	R_{1p}-R_{1d}[a]/ms^{-1}
7.148	172.6
4.279	87.96
1.872	42.37
0.745	12.86
0.511	7.492
0.397	5.110
0.248	2.020
0.200	1.768
0.111	0.704
0.100	0.557
0.074	0.404
0.049	0.277
0.037	0.157
0.010	0.009

Table 2S: Proton relaxivities for a 0.2 mM [Gd(EPTPA-C16)(H_2O)]$^{2-}$ solution (non aggregated form).

Frequency/MH	37ºC	25ºC	5ºC
20.00	6.68	9.11	14.38
14.80	6.78	9.75	15.07
10.90	7.30	11.08	14.77
8.03	7.91	11.62	16.01
5.93	9.23	12.56	17.77
4.37	9.99	13.14	18.61
3.23	10.91	14.32	19.81
2.38	11.75	15.59	21.17
1.76	12.49	15.97	21.67
1.30	13.07	16.78	21.82
0.96	13.46	16.97	21.98
0.71	13.75	17.03	22.29
0.52	13.99	17.06	22.37
0.38	14.17	17.09	22.55
0.28	14.22	17.09	22.55
0.21	14.38	17.09	22.54
0.15	14.43	17.06	22.57
0.11	14.51	17.22	22.59
0.08	14.54	17.03	22.54
0.06	14.67	17.06	22.51
0.05	14.57	17.09	22.56
0.03	14.62	17.09	22.61
0.03	14.75	17.09	22.60
0.02	14.78	17.06	22.56
0.01	14.78	17.06	22.56
0.01	14.78	17.06	22.55
30.00	6.61	8.79	14.02
40.00	6.58	8.96	15.03
60.00	6.53	8.78	15.00
200.00	6.30	8.62	12.09

Table 3S: Proton relaxivities in 2 mM [Gd(EPTPA-C16)(H_2O)]$^{2-}$

	37ºC	**25ºC**	**5ºC**
20.00	12.73	19.73	35.79
14.76	11.78	18.50	32.14
10.89	11.16	17.22	28.20
8.03	10.85	15.88	24.94
5.93	10.62	14.67	21.55
4.37	10.45	14.07	20.19
3.23	10.79	14.25	20.05
2.38	11.47	15.02	20.75
1.76	11.95	15.77	21.70
1.30	12.54	16.57	22.69
0.96	13.05	17.28	23.72
0.71	13.37	17.85	24.65
0.52	13.66	18.35	25.25
0.38	13.86	18.68	25.72
0.28	13.94	18.82	26.14
0.21	14.05	18.97	26.34
0.15	14.09	19.03	26.54
0.11	14.07	19.05	26.55
0.08	14.06	19.12	26.54
0.06	14.10	19.08	26.62
0.05	14.13	19.17	26.55
0.03	14.05	19.15	26.62
0.02	14.09	19.12	26.67
0.02	14.13	19.17	26.55
0.01	14.15	19.13	26.60
0.01	14.09	19.17	26.57
30.00	14.87	21.42	35.84
40.00	14.94	21.88	34.39
60.00	14.10	19.84	26.79
200.00	8.49	9.23	10.11
400.00	5.10	5.69	6.38

Table 4S: Proton relaxivities resulting from the micellar form calculated using the equation $r_1^a = \left(R_1^{obs} - R_1^d - r_1^{n.a.} \times cmc\right)/\left(c_{Gd} - cmc\right)$.

Frequency/MHz	5ºC	25ºC	37ºC
20.000	40.17	21.91	13.97
14.800	35.63	20.29	12.80
10.900	30.95	18.47	11.95
8.030	26.76	16.76	11.45
5.930	22.33	15.10	10.91
4.370	20.51	14.26	10.54
3.230	20.10	14.24	10.76
2.380	20.67	14.90	11.41
1.760	21.71	15.73	11.84
1.300	22.86	16.52	12.44
0.956	24.08	17.35	12.97
0.706	25.14	18.02	13.29
0.521	25.84	18.61	13.60
0.384	26.37	19.01	13.79
0.283	26.87	19.17	13.88
0.209	27.11	19.35	13.98
0.154	27.35	19.44	14.02
0.114	27.37	19.42	13.98
0.084	27.35	19.54	13.97
0.062	27.45	19.50	13.99
0.046	27.37	19.59	14.03
0.034	27.45	19.57	13.93
0.025	27.51	19.53	13.96
0.018	27.37	19.60	14.00
0.014	27.43	19.56	14.03
0.010	27.39	19.60	13.95
30.000	40.30	24.01	16.56
40.000	38.35	24.52	16.65
60.000	29.20	22.11	15.65
200.00	9.71	9.36	8.94

Table 5S: Variable temperature reduced transverse and longitudinal ^{17}O relaxation rates and chemical shifts of $[Gd(EPTPA\text{-}C16)(H_2O)]^{2-}$ solution at 9.4T. $c_{Gd} = 26{,}77mmol/Kg$; $P_m = 4.81\times10^{-4}$

T/K	1000/T	T_1/s (ref)	T_1/s	$\ln(1/T_{1r})$	T_2/s (ref)	T_2/s	$\ln(1/T_{2r})$	ref /Hz	frec /Hz	$\Delta\omega_r$ /Hz
308.1	3.25	9.64E-03	6.94E-03	11.34	9.09E-03	3.89E-03	12.63	447.7	393.9	-7.03E+05
287.0	3.48	5.32E-03	4.03E-03	11.74	5.39E-03	2.11E-03	13.30	495.3	440.6	-7.16E+05
293.8	3.40	6.45E-03	4.86E-03	11.57	6.47E-03	2.63E-03	13.06	483.2	421.8	-8.02E+05
300.6	3.33	7.66E-03	5.64E-03	11.49	7.80E-03	3.29E-03	12.81	462.8	400.5	-8.15E+05
314.1	3.18	1.10E-02	8.22E-03	11.08	1.03E-02	4.87E-03	12.33	436.3	378.2	-7.60E+05
281.0	3.56	4.31E-03	3.23E-03	11.99	4.32E-03	1.76E-03	13.46	513.4	455.8	-7.53E+05
274.5	3.64	3.39E-03	2.71E-03	11.94	3.46E-03	1.46E-03	13.62	533.7	478.7	-7.19E+05

Table 6: Variable temperature reduced transverse and longitudinal ^{17}O relaxation rates and chemical shifts of $[Gd(EPTPA\text{-}C16)(H_2O)]^{2-}$ solution at 4.7T. $c_{Gd} = 26.77mmol/kg$; $P_m = 4.81\times10^{-4}$.

T/K	1000/T	T_1/s (ref)	T_1/s	$\ln(1/T_{1r})$	T_2/s (ref)	T_2/s	$\ln(1/T_{2r})$	ref /Hz	frec /Hz	$\Delta\omega_r$ /Hz
306.6	3.26	8.98E-03	6.52E-03	11.38	8.95E-03	4.05E-03	12.55	-529. 9	-556.7	-3.51E+05
279.8	3.57	4.07E-03	2.85E-03	12.30	4.05E-03	1.70E-03	13.48	-497.4	-520.3	-2.99E+05
287.8	3.47	5.38E-03	3.71E-03	12.07	5.35E-03	2.19E-03	13.24	-506.5	-530.8	-3.18E+05
297.2	3.36	7.05E-03	4.98E-03	11.72	6.97E-03	2.99E-03	12.89	-515.8	-544.8	-3.79E+05
316.1	3.16	1.11E-02	8.41E-03	10.99	1.10E-02	5.34E-03	12.21	-540.5	-566.8	-3.44E+05
325.2	3.08	1.34E-02	1.04E-02	10.70	1.32E-02	6.96E-03	11.86	-554.7	-578.6	-3.12E+05
271.3	3.69	2.91E-03	2.19E-03	12.36	2.91E-03	1.31E-03	13.68	-485.8	-506.9	-2.76E+05